A molecular biomarker for end-Permian plant extinction in South China

Chunjiang Wang[1]* and Henk Visscher[2]*

[1]College of Geosciences, and State Key Laboratory of Petroleum Resources and Prospecting, China University of Petroleum (Beijing), Beijing 102249, China
[2]Faculty of Geosciences, Utrecht University, 3584CS Utrecht, The Netherlands

ABSTRACT

To help resolve current controversies surrounding the fundamental question of synchrony between end-Permian mass extinction on land and in the sea, we examined the marine Permian–Triassic reference section at Meishan (southeastern China) for land-derived molecular degradation products of pentacyclic triterpenoids with oleanane carbon skeletons, diagnostic for the Permian plant genus *Gigantopteris*. We identified a continuous quantitative record of mono-aromatic *des*-A-oleanane, which abruptly ends in the main marine extinction interval just below the Permian-Triassic boundary. This taxon-specific molecular biomarker, therefore, reveals in unmatched detail the timing and tempo of the demise of one of the most distinctive Permian plants and provides evidence of synchronous extinction among continental and marine organisms. Parallel reduction in the relative abundance of lignin phenols confirms that aridity-driven extinction was not restricted to *Gigantopteris* but likely affected the entire wetland flora of the equatorial South China microcontinent.

INTRODUCTION

Multiple lines of paleontological, geochemical, and sedimentological evidence confirm worldwide collapse of continental and marine ecosystems at the end of the Permian Period. However, there are conflicting views on the question of synchrony of the associated mass extinctions. Global meta-analysis of the temporal distribution of Permian and Triassic plant fossils may suggest that evidence for mass extinction among land plants is far from robust (Nowak et al., 2019), and regional studies commonly conclude that continental and marine extinctions were timed differently (e.g., Fielding et al., 2019). The resolution of the temporal relationship between extinctions on land and in the sea is necessary to fully understand the cause of the end-Permian biotic crisis.

Disagreements about extinction synchrony are at least partly related to imprecise correlation of continental fossil records to the marine Global Stratotype Section and Point (GSSP) for the base of the Triassic at Meishan, Zhejiang Province in southeastern China (Yin et al., 2001). Besides hosting the conodont-defined

Permian-Triassic boundary, Meishan section D serves as the principal global reference profile for biological, chemical, and physical signatures of the end-Permian biotic crisis. Starting at the base of bed 25, a profound loss of faunal biodiversity defines the main marine extinction interval, bracketed by high-precision U-Pb zircon dates between 251.941 ± 0.037 Ma and 251.880 ± 0.031 Ma (Burgess et al., 2014; Chen et al., 2015). Molecular studies have demonstrated significant influx of plant and bacterial organic matter, reflecting ecosystem collapse on land (e.g., Wang, 2007; Wang and Visscher, 2007; Nabbefeld et al., 2010; Kaiho et al., 2016). However, the Meishan section does not contain a record of physical plant fossils suitable for direct temporal correlation of continental and marine patterns of taxic extinction. Plant macrofossils are absent, and latest Permian palynomorph assemblages are dominated by marine phytoplankton (acritarchs), with only a subordinate and inconclusive record of spores and pollen of land plants (Ouyang and Utting, 1990).

The Meishan section is paleogeographically situated on the South China tectonic block, a microcontinent in the easternmost Paleo-Tethys Ocean, largely covered by sea during the Permian-Triassic transition. Floristically, the

remaining islands were the domain of the classic late Permian *Gigantopteris* wetland flora, the final phase in the development of the Pennsylvanian–Permian Cathaysian floral province of East Asia. Macrofossil and spore-pollen records have been analyzed from multiple boundary sections deposited in fluvial and coastal settings, particularly in the provinces of Guizhou and Yunnan in southwestern China (e.g., Ouyang, 1982; Peng et al., 2006; Yu et al., 2015; Chu et al., 2016; Feng et al., 2020a, 2020b). By using magnetostratigraphy, isotope stratigraphy, and U-Pb geochronology of interbedded volcanic ash layers, plant records have been correlated to the Meishan section (e.g., Zhang et al., 2016). Although there is little doubt about a marked floral turnover, these correlations offer conflicting views as to whether the timing of eventual extinction of the genus *Gigantopteris* and other characteristic taxa of the *Gigantopteris* flora preceded, paralleled, or succeeded the end-Permian marine extinctions. In this study, we demonstrate that the molecular remnants of land plants preserved in the GSSP section shed new light on temporal links between continental and marine bioevents, providing an effective solution to this uncertainty.

CHEMOTAXONOMIC BACKGROUND

Gigantopteris has been established as a fossil genus for megaphyllous leaves with a remarkable angiosperm-like physiognomy and venation pattern (e.g., Glasspool et al., 2004). Along with morphologically similar Permian genera from East Asia and North America, differing in details of gross leaf architecture and venation, *Gigantopteris* may be grouped in the polyphyletic order Gigantopteridales. Jointly with the genus *Gigantonoclea*, however, *Gigantopteris* may cover a narrow monophyletic taxon. Liana-like stems associated with these genera share the earliest known secondary xylem with

*E-mail: wchj333@126.com; h.visscher@uu.nl

high-conductivity vessel conduits (Li et al., 1996), but conclusive information regarding the structure of reproductive organs, essential in resolving the phylogenetic position of fossil gymnosperms, is still lacking. The morphology of gigantopterid pollen grains is elusive, precluding the detection of *Gigantopteris* in spore-pollen records.

In addition to morphological and anatomical similarities, the most startling resemblance of *Gigantopteris* and *Gigantonoclea* with angiosperms is the presence of oleanane-type molecular compounds (Taylor et al., 2006). Oleanane represents the most common carbon skeleton for the synthesis of pentacyclic-triterpenoid secondary metabolites presently produced by a wide variety of angiosperms as chemical protection

and defense against herbivores, pests, and pathogens (e.g., Wink, 2016). Except for a record of oleanolic acid in *Pinus massoniana*, oleanane is unknown from extant gymnosperms (Si et al., 2017); among extinct gymnosperms, it is also found in some Mesozoic Bennettitales (Taylor et al., 2006). The source of Carboniferous oleanane in North America is still unknown (Philp et al., 2021). Although secondary metabolites do not necessarily carry phylogenetic information (Wink, 2016), among the Permian plants in South China the compound may serve as a useful chemotaxonomic character to diagnose the *Gigantopteris-Gigantonoclea* combination. For taxonomic convenience, we here refer to this grouping as *Gigantopteris*. The presence or absence of oleanane in other gigantopterid genera

from southeastern Asia and North America still needs to be determined.

Modern soil organic matter commonly contains angiosperm-derived oleananes or their diagenetic derivatives (e.g., Jaffé et al., 1996; Otto and Simpson, 2005; He et al., 2018). Likewise, soils of the Permian *Gigantopteris* forests could have contained aliphatic or aromatized degradation products of oleanane precursors. Because continentally sourced organic carbon in marine sediments is typically predominated by soil-derived constituents (Regnier et al., 2013), we hypothesize that the Meishan organic assemblage may well include a record of gigantopterid molecular biomarkers, suggesting the precise timing of end-Permian plant extinction on the South China microcontinent. We selected 88
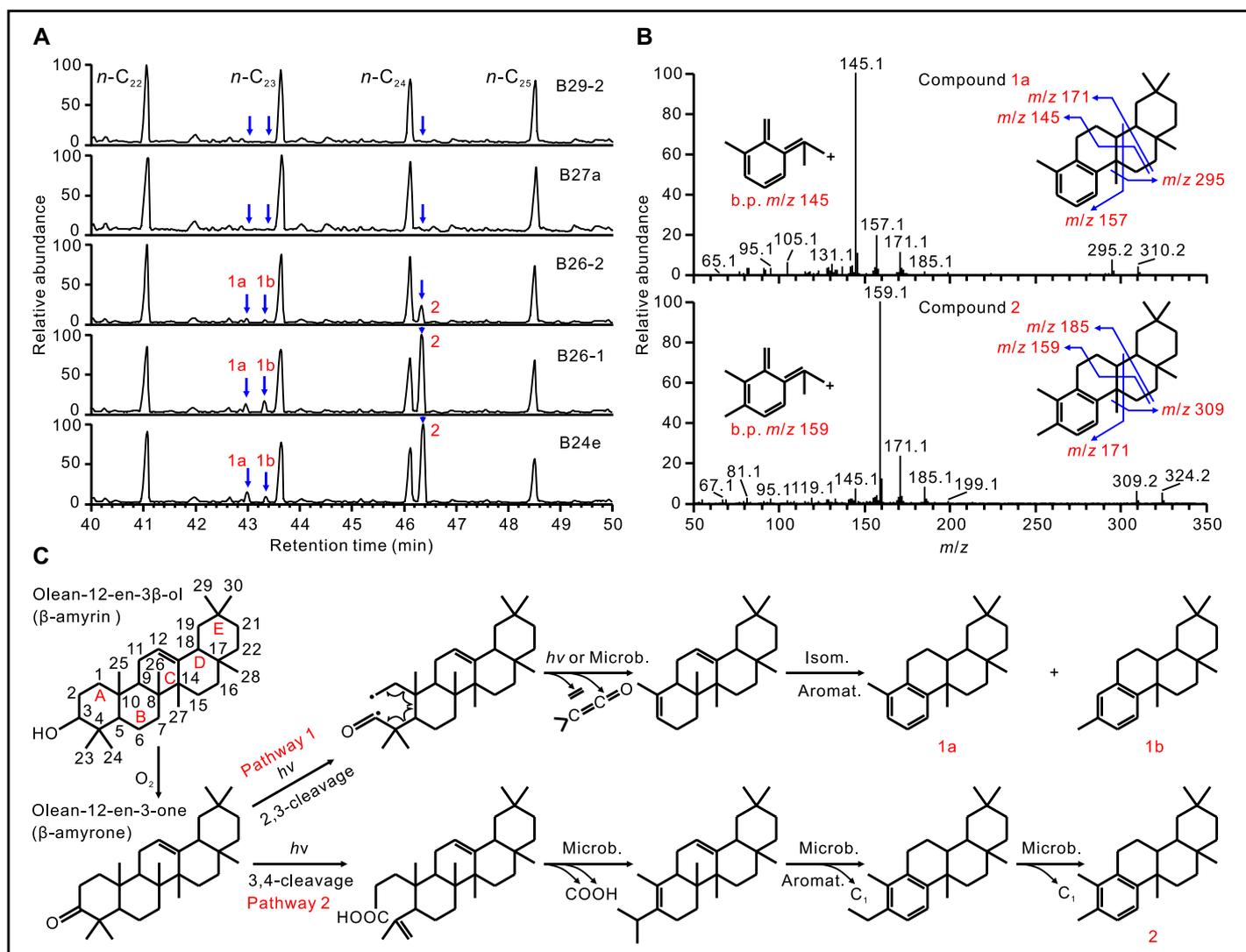
Figure 1. Identification and genesis of mono-aromatic *des*-A-oleananes (MADAO). (A) Mass chromatograms (*m/z* 85 + *m/z* 145 + *m/z* 159; *m/z*—ratio of mass to charge) of five successive samples (from bottom to top), exemplifying the dramatic decline of relative abundances of compounds 1a, 1b, and 2 across the Permian-Triassic boundary interval (beds 24 – 29; see Figs. 2 and 3) at Meishan, southeastern China. (B) Mass spectra and proposed structure elucidation for compounds 1a and 2. Base peak (b.p.) ions at *m/z* 145 and *m/z* 159 can be rationalized as result of C- and D-ring cleavage. Compounds 1a-1b and 2 can be tentatively classified as C$_{23}$ *des*-A-26-norolean-5,7,9-triene and C$_{24}$ *des*-A-26-norolean-5,7,9-triene, respectively. (C) Proposed diagenetic pathways for derivation of compounds 1a-1b and 2 from β-amyrin via 2,3-cleavage (pathway 1) or 3,4-cleavage (pathway 2), followed by degradation of side chains and B-ring aromatization. *hv* denotes photochemical transformation. Aromat.—aromatization; Isom.—isomerization; Microb.—microbial.

samples, collected from Meishan sections B, C, and D (Yin et al., 2001), for organic-geochemical analysis (see the Supplemental Material[1] for analytical procedures and the data set).

RESULTS AND DISCUSSION
Identification of a Taxon-Specific Biomarker

Gas chromatography–mass spectrometry (GC-MS) allowed the detection of at least three distinct mono-aromatic tetracyclic hydrocarbon compounds, eluting before n-C_{23} alkanes (isomeric compounds 1a and 1b) and after n-C_{24} (compound 2; Fig. 1A). We have interpreted the compounds as mono-aromatic *des*-A-oleananes (MADAO; see the Supplemental Material). We used the mass-spectral characteristics (Fig. 1B), supplemental analysis of organic matter from the Oligocene Baigang Formation in southern China (Fig. S1 in the Supplemental Material), and published concepts about structure and formation of A-ring degraded pentacyclic triterpenoids (e.g., Trendel et al., 1989; Stout, 1992; Eiserbeck et al., 2012; He et al., 2018; Asahi and Sawada, 2019).

Oleanane and its diagenetic transformation products have long been used to identify angiosperm-derived organic matter input in Late Cretaceous to recent sediments (e.g., Moldowan et al., 1994). Given the presence of oleanane in *Gigantopteris*, MADAO can also be taken as an age-related, taxon-specific biomarker, indicative of a prominent late Permian floral element. Aromatic *des*-A-triterpenoids derived from oleanane precursors have been detected in soils of mangroves (He et al., 2018) and periodically flooded rainforests (Jaffé et al., 1996), suggesting that these relatively stable compounds are formed under anaerobic conditions in temporarily submerged soils. Their occurrence in surface soils confirms fast diagenetic reactions early during litter decay and substantiates the assumption that MADAO was exported to the sea after a short residence in soils.

Temporal Distribution of MADAO

We restrict our analysis of the temporal variation of MADAO to the stratigraphic distribution of compound 2 because its relative abundance is distinctly higher than that of compounds 1a and 1b (Fig. 1A). Starting in bed 23 in the Changxing Formation, this variation correlates to the quantitative record of monomeric phenols derived from kerogen pyrolysates, which likely reflects influx of lignin or altered lignin of vascular plants (Wang and Visscher, 2007; Fig. 2).

Following a sharp decline of MADAO in bed 26, further upsection in the Yinkeng Formation the compound is absent or remains restricted to trace amounts, probably derived from transgressive reworking (Fig. 3). The lignin phenols clearly mirror this decline but then remain pres-
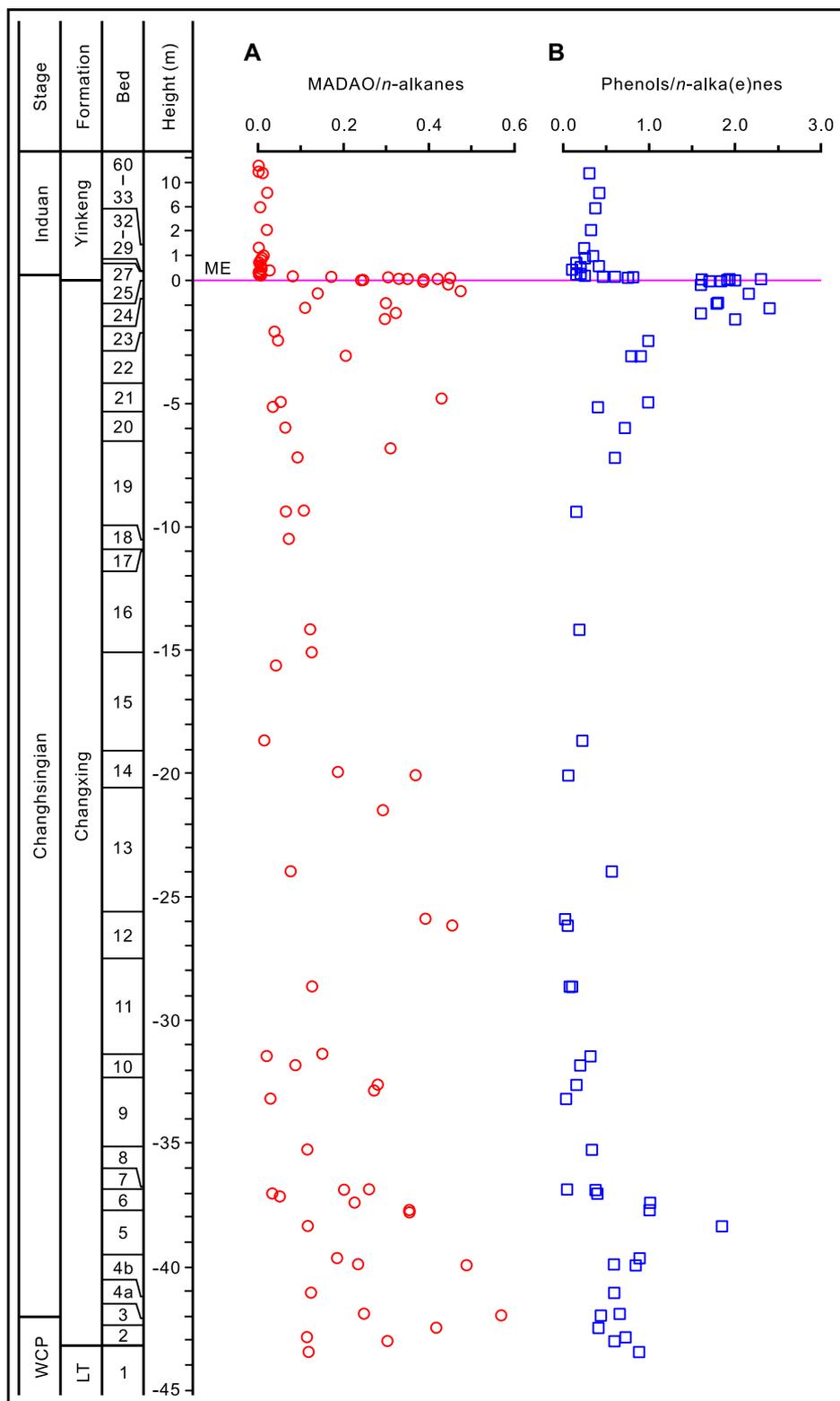
Figure 2. Temporal pattern of mono-aromatic *des*-A-oleananes (MADAO) and phenol indices across the Changxing and Yinkeng Formations at Meishan, southeastern China. (A) Ratio of MADAO to *n*-alkanes. (B) Ratio of phenols to *n*-alka(e)nes. Note the different scale for the upper part of the column. For precise position of data points, sample lithology, index quantification, and biomarker relative abundance values, see the Supplemental Material (see footnote 1). WCP—Wuchiapingian Stage; LT—Longtan Formation; ME—onset marine mass extinction.
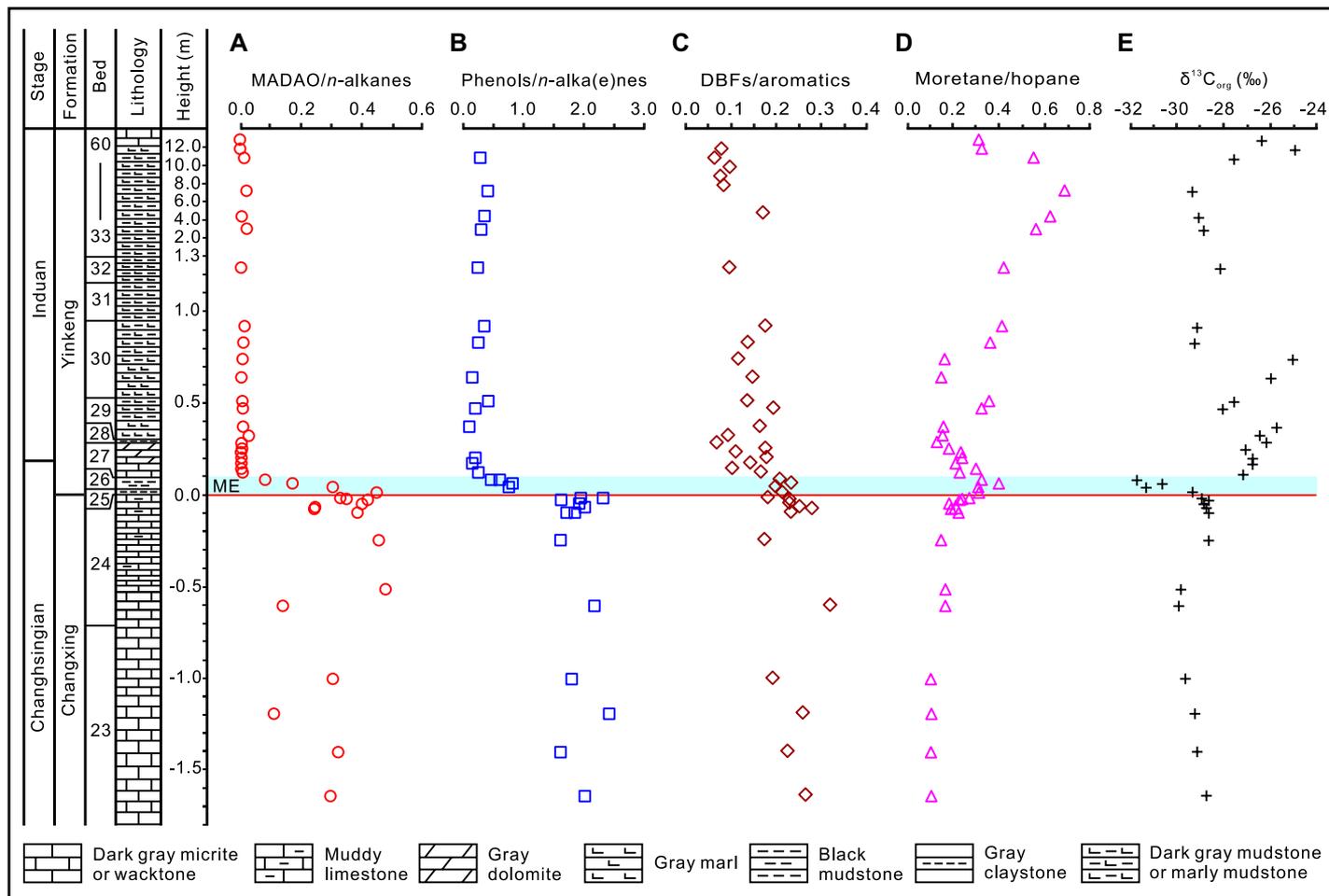
Figure 3. Profiles of terrigenous molecular biomarker indices and organic-matter δ¹³C (δ¹³C$_{org}$) values across Permian-Triassic transition at Meishan. (A) Ratio of mono-aromatic *des*-A-oleananes (MADAO) to *n*-alkanes. (B) Ratio of phenols to *n*-alka(e)nes. (C) Ratio of dibenzofurans (DBFs) to total aromatics. (D) Ratio of moretanes to hopanes. (E) Kerogen organic-carbon isotope ratio. Note the different scale for the upper part of the column. For precise position of data points, sample lithology, index quantification, and biomarker relative abundance values, see the Supplemental Material (see footnote 1). ME—onset marine mass extinction; blue zone indicates interval of terrestrial ecosystem collapse, floral turnover, and extinction.

ent in minor concentrations. Other land-derived organic constituents show a different pattern. Elevated concentrations of dibenzofurans (DBFs; Fig. 3C), probably originating from soil polysaccharides, such as cellulose and hemicellulose (Sephton et al., 2005; Wang and Visscher, 2007), continue to prevail in the Yinkeng Formation. There is no correlation to peak occurrences of polycyclic aromatic hydrocarbons indicative of anomalous wildfire activity (Nabbefeld et al., 2010). In bed 24, the onset of a fluctuating pattern of generally elevated moretane/hopane ratios may point to a raised input of βα-hopanoid metabolites from soil bacteria (Wang, 2007; Fig. 3D). The end of the MADAO record corresponds to the δ¹³C$_{org}$ (org—organic matter) minimum in bed 26 (Fig. 3E).

Extinction of the *Gigantopteris* Flora

The decline and termination of the continuous MADAO record in bed 26 clearly depicts the timing and tempo of the end-Permian extinction of *Gigantopteris* in South China. The extinction was synchronous with the main marine extinction event at Meishan. Because the Permian-Triassic boundary is defined in the middle of bed 27, the molecular fossils independently contradict claims of temporal persistence of *Gigantopteris* into the Triassic (e.g., Nowak et al., 2019). Age estimates of bed 26 (ca. 251.933–251.912 Ma; Chen et al., 2015) suggest that extinction is constrained to a short episode of ∼21 k.y.

In forested ecosystems, the subaerial and subsurface biomass of canopy trees is the vital determining factor of the lignin content of soil organic matter. Present-day deforestation generally results in significantly decreased lignin yields together with a relative increase of cellulose and hemicellulose (Kroeger et al., 2018). On the basis of anatomical characteristics (narrow stems, large vessel diameters, massive leaves), the *Gigantopteris* plants should be interpreted as canopy lianas rather than canopy trees (Li et al., 1996). Consequently, the drastically reduced abundance of lignin phenols

in bed 26 implies that not only *Gigantopteris* but especially dominant tree-forming floral elements must have ended their contribution to the soil organic carbon stock. The macrofossil and spore-pollen records from Guizhou and Yunnan Provinces suggest that in addition to species of Calamitales (equisetophytes), Lepidodendrales (lycophytes), and Noeggerathiales (progymnosperms), the overall tree canopy of the wetland forests was composed mainly of marattialean tree ferns belonging to the extinct family Psaroniaceae (see the Supplemental Material). In a global perspective, therefore, the lignin phenol record at Meishan strengthens the evidence base for the end-Permian *coup de grâce* to the iconic arborescent spore plants that long dominated the canopy of tropical peat forests during later Paleozoic times.

Beginning in bed 23, accelerated deforestation and ensuing soil erosion is well reflected in the intensified burial flux of lignin phenols, dibenzofurans, and soil-bacterial moretanes (Fig. 3). The macrofossil and spore-pollen

assemblages from southwestern China provide evidence that concurrently with deforestation and the cessation of peat formation, the *Gigantopteris* flora was rapidly replaced by low-biomass, drought-tolerant plants (e.g., Ouyang, 1982; Peng et al., 2006; Yu et al., 2015; Chu et al., 2016; Feng et al., 2020a, 2020b). The low-shrub peltasperm *Germaropteris* and the succulent lycophyte *Lepacyclotes* may have pioneered this later flora. Although other, globally operating environmental stress factors (acidification, ultraviolet B radiation, mercury toxicity) have likely contributed to continental ecosystem collapse, the colonizing flora affirms intensified seasonal water stress as the main proximal trigger of end-Permian deforestation. In modern forested ecosystems, droughts accompanied by raised temperatures resulting from anthropogenic CO_2 forcing are known to instigate marked increases in tree mortality rates (e.g., Allen et al., 2015). At Meishan, the inception of deforestation matches the onset of the globally identified, negative carbonate-isotope ($\delta^{13}C_{carb}$) excursion (Burgess et al., 2014). Consistent with a scenario of global warming, probably driven by Siberian Traps igneous activity, this correspondence may support a causal link between massive injection of ^{13}C-depleted CO_2 into the atmosphere and aridity-driven die-off of the *Gigantopteris* flora in the South China archipelago.

CONCLUSION

Continuous records of land-derived biomarkers have become a powerful tool for reconstructing the ecology of deep-time mass-extinction events (Whiteside and Grice, 2016). Our present analysis of MADAO illustrates, for the first time, the great potential of biomarkers with narrow taxon specificity to detect extinction itself. Moreover, these molecular fossils can reduce the bias in the assessment of tempo and timing of end-Permian plant extinction imposed by chance-dependent last occurrences of conventional fossils.

It would be premature to conclude that the spatiotemporal correspondence between continental and marine extinctions demonstrated for the Cathaysian floristic realm can serve as a reference point for affirming concepts of synchronous end-Permian extinction worldwide. Nevertheless, we believe that molecular biomarker data from the Meishan GSSP section provide ample grounds for rethinking conflicting interpretations of plant fossil records from the Gondwanan, Angaran, and Euramerican floral provinces.

REFERENCES CITED

Allen, C.D., Breshears, D.D., and McDowell, N.G., 2015, On underestimation of global vulnerability to tree mortality and forest die-off from hotter drought in the Anthropocene: Ecosphere, v. 6, 129, https://doi.org/10.1890/ES15-00203.1.

Asahi, H., and Sawada, K., 2019, GC–MS analyses of ring degraded triterpenoids in event deposits: Researches in Organic Geochemistry, v. 35, p. 55–72, https://doi.org/10.20612/rog.35.2_55 (in Japanese with English abstract).

Burgess, S.D., Bowring, S., and Shen, S.-Z., 2014, High-precision timeline for Earth's most severe extinction: Proceedings of the National Academy of Sciences of the United States of America, v. 111, p. 3316–3321, https://doi.org/10.1073/pnas.1317692111.

Chen, Z.-Q., et al., 2015, Complete biotic and sedimentary records of the Permian–Triassic transition from Meishan section, South China: Ecologically assessing mass extinction and its aftermath: Earth-Science Reviews, v. 149, p. 67–107, https://doi.org/10.1016/j.earscirev.2014.10.005.

Chu, D., Yu, J., Tong, J., Benton, M.J., Song, H., Huang, Y., Song, T., and Tian, L., 2016, Biostratigraphic correlation and mass extinction during the Permian-Triassic transition in continental-marine siliciclastic settings of South China: Global and Planetary Change, v. 146, p. 67–88, https://doi.org/10.1016/j.gloplacha.2016.09.009.

Eiserbeck, C., Nelson, R.K., Grice, K., Curiale, J., and Reddy, C.M., 2012, Comparison of GC–MS, GC–MRM-MS, and GC × GC to characterise higher plant biomarkers in Tertiary oils and rock extracts: Geochimica et Cosmochimica Acta, v. 87, p. 299–322, https://doi.org/10.1016/j.gca.2012.03.033.

Feng, Z., Wei, H.-B., Guo, Y., He, X.-Y., Sui, Q., Zhou, Y., Liu, H.-Y., Gou, X.-D., and Lv, Y., 2020a, From rainforest to herbland: New insights into land plant responses to the end-Permian mass extinction: Earth-Science Reviews, v. 204, 103153, https://doi.org/10.1016/j.earscirev.2020.103153.

Feng, Z., Wei, H.-B., Ye, R.-H., Sui, Q., Gou, X.-D., Guo, Y., Liu, L.-J., and Yang, S.-L., 2020b, Latest Permian peltasperm plant from Southwest China and its paleoenvironmental implications: Frontiers of Earth Science, v. 8, 450, https://doi.org/10.3389/feart.2020.559430.

Fielding, C.R., et al., 2019, Age and pattern of the southern high-latitude continental end-Permian extinction constrained by multiproxy analysis: Nature Communications, v. 10, 385, https://doi.org/10.1038/s41467-018-07934-z.

Glasspool, I.J., Hilton, J., Collinson, M.E., and Wang, S.-J., 2004, Defining the gigantopterid concept: A reinvestigation of *Gigantopteris* (*Megalopteris*) *nicotianaefolia* Schenck and its taxonomic implications: Palaeontology, v. 47, p. 1339–1361, https://doi.org/10.1111/j.0031-0239.2004.00425.x.

He, D., Simoneit, B.R.T., Cloutier, J.B., and Jaffé, R., 2018, Early diagenesis of triterpenoids derived from mangroves in a subtropical estuary: Organic Geochemistry, v. 125, p. 196–211, https://doi.org/10.1016/j.orggeochem.2018.09.005.

Jaffé, R., Elismé, T., and Cabrera, A.C., 1996, Organic geochemistry of seasonally flooded rain forest soils: Molecular composition and early diagenesis of lipid components: Organic Geochemistry, v. 25, p. 9–17, https://doi.org/10.1016/S0146-6380(96)00103-9.

Kaiho, K., et al., 2016, Effects of soil erosion and anoxic–euxinic ocean in the Permian–Triassic marine crisis: Heliyon, v. 2, e00137, https://doi.org/10.1016/j.heliyon.2016.e00137.

Kroeger, M.E., et al., 2018, New biological insights into how deforestation in Amazonia affects soil microbial communities using metagenomics and metagenome-assembled genomes: Frontiers in Microbiology, v. 9, 1635, https://doi.org/10.3389/fmicb.2018.01635.

Li, H., Taylor, E.L., and Taylor, T.N., 1996, Permian vessel elements: Science, v. 271, p. 188–189, https://doi.org/10.1126/science.271.5246.188.

Moldowan, J.M., Dahl, J., Huizinga, B.J., Fago, F.J., Hickey, L.J., Peakman, T.M., and Taylor, D.W., 1994, The molecular fossil record of oleanane and its relation to angiosperms: Science, v. 265, p. 768–771, https://doi.org/10.1126/science.265.5173.768.

Nabbefeld, B., Grice, K., Summons, R.E., Hays, L.E., and Cao, C., 2010, Significance of polycyclic aromatic hydrocarbons (PAHs) in Permian/Triassic boundary sections: Applied Geochemistry, v. 25, p. 1374–1382, https://doi.org/10.1016/j.apgeochem.2010.06.008.

Nowak, H., Schneebeli-Hermann, E., and Kustatscher, E., 2019, No mass extinction for land plants at the Permian–Triassic transition: Nature Communications, v. 10, 384, https://doi.org/10.1038/s41467-018-07945-w.

Otto, A., and Simpson, M.J., 2005, Degradation and preservation of vascular plant-derived biomarkers in grassland and forest soils from western Canada: Biogeochemistry, v. 74, p. 377–409, https://doi.org/10.1007/s10533-004-5834-8.

Ouyang, S., 1982, Upper Permian and Lower Triassic palynomorphs from eastern Yunnan, China: Canadian Journal of Earth Sciences, v. 19, p. 68–80, https://doi.org/10.1139/e82-006.

Ouyang, S., and Utting, J., 1990, Palynology of upper Permian and lower Triassic rocks, Meishan, Changxing County, Zhejiang Province, China: Review of Palaeobotany and Palynology, v. 66, p. 65–103, https://doi.org/10.1016/0034-6667(90)90029-I.

Peng, Y., Yu, J., Gao, Y., and Yang, F., 2006, Palynological assemblages of non-marine rocks at the Permian–Triassic boundary, western Guizhou and eastern Yunnan, South China: Journal of Asian Earth Sciences, v. 28, p. 291–305, https://doi.org/10.1016/j.jseaes.2005.10.007.

Philp, P., Wood, M., Gorenekli, Y.S., Nguyen, T., Symcox, C., Wang, H., and Kim, D., 2021, The presence of 18α(H)-oleanane in Pennsylvanian and Mississippian rocks in the Anadarko Basin, Oklahoma: Organic Geochemistry, v. 152, 104181, https://doi.org/10.1016/j.orggeochem.2021.104181.

Regnier, P., et al., 2013, Anthropogenic perturbation of the carbon fluxes from land to ocean: Nature Geoscience, v. 6, p. 597–607, https://doi.org/10.1038/ngeo1830.

Sephton, M.A., Looy, C.V., Brinkhuis, H., Wignall, P.B., de Leeuw, J.W., and Visscher, H., 2005, Catastrophic soil erosion during the end-Permian biotic crisis: Geology, v. 33, p. 941–944, https://doi.org/10.1130/G21784.1.

Si, C.-L., Gao, Y., Wu, L., Liu, R., Wang, G., Dai, L., Li, X., and Hong, Y., 2017, Isolation and characterization of triterpenoids from the stem barks of *Pinus massoniana*: Holzforschung, v. 71, p. 697–703, https://doi.org/10.1515/hf-2016-0228.

Stout, S.A., 1992, Aliphatic and aromatic triterpenoid hydrocarbons in a Tertiary angiospermous lignite: Organic Geochemistry, v. 18, p. 51–66, https://doi.org/10.1016/0146-6380(92)90143-L.

Taylor, D.W., Li, H., Dahl, J., Fago, F.J., Zinniker, D., and Moldowan, J.M., 2006, Biogeochemical

evidence for the presence of the angiosperm molecular fossil oleanane in Paleozoic and Mesozoic non-angiospermous fossils: Paleobiology, v. 32, p. 179–190, https://doi.org/10.1666/0094-8373(2006)32[179:BEFTPO]2.0.CO;2.

Trendel, J.M., Lohmann, F., Kintzinger, J.P., Albrecht, P., Chiarone, A., Riche, C., Cesario, M., Guilhem, J., and Pascard, C., 1989, Identification of *des*-A-triterpenoid hydrocarbons occurring in surface sediments: Tetrahedron, v. 45, p. 4457–4470, https://doi.org/10.1016/S0040-4020(01)89081-5.

Wang, C., 2007, Anomalous hopane distributions at the Permian–Triassic boundary, Meishan, China—Evidence for the end-Permian marine ecosystem collapse: Organic Geochemistry, v. 38, p. 52–66, https://doi.org/10.1016/j.orggeochem.2006.08.014.

Wang, C., and Visscher, H., 2007, Abundance anomalies of aromatic biomarkers in the Permian–Triassic boundary section at Meishan, China—Evidence of end-Permian terrestrial ecosystem collapse: Palaeogeography, Palaeoclimatology, Palaeoecology, v. 252, p. 291–303, https://doi.org/10.1016/j.palaeo.2006.11.048.

Whiteside, J.H., and Grice, K., 2016, Biomarker records associated with mass extinction events: Annual Review of Earth and Planetary Sciences, v. 44, p. 581–612, https://doi.org/10.1146/annurev-earth-060115-012501.

Wink, M., 2016, Evolution of secondary plant metabolism, *in* eLS: Chichester, John Wiley & Sons, https://doi.org/10.1002/9780470015902.a0001922.pub3.

Yin, H., Zhang, K., Tong, J., Yang, Z., and Wu, S., 2001, The Global Stratotype Section and Point (GSSP) of the Permian-Triassic boundary: Episodes, v. 24, p. 102–114, https://doi.org/10.18814/epiiugs/2001/v24i2/004.

Yu, J., Broutin, J., Chen, Z.-Q., Shi, X., Li, H., Chu, D., and Huang, Q., 2015, Vegetation changeover across the Permian–Triassic Boundary in Southwest China: Extinction, survival, recovery and palaeoclimate: A critical review: Earth-Science Reviews, v. 149, p. 203–224, https://doi.org/10.1016/j.earscirev.2015.04.005.

Zhang, H., Cao, C.-Q., Liu, X.-L., Mu, L., Zheng, Q.-F., Liu, F., Xiang, L., Liu, L.-J., and Shen, S.-Z., 2016, The continental end–Permian mass extinction in South China: Palaeogeography, Palaeoclimatology, Palaeoecology, v. 448, p. 108–124, https://doi.org/10.1016/j.palaeo.2015.07.002.

Printed in USA